Spherical Expanding Flame in Silane-Hydrogen-Nitrous Oxide Mixtures

Pauline Vervish-Kljakic[1], Rémy Mével[1], Nabiha Chaumeix[2], Gabrielle Dupré[2], Claude-Étienne Paillard[2], Mathieu Allix[3], Nasser Darabiha[4], Joseph Shepherd[1]

[1]California Institute of Technology, Pasadena, USA
[2]ICARE, CNRS, Orléans, France
[3]CEMHTI, CNRS, Orléans, France
[4]Laboratoire EM2C-CNRS UPR 288, École Centrale Paris, Châtenay-Malabry, France

1 Introduction

Silane-based mixtures, such as silane-nitrous oxide blends, are mainly used in the semi-conductor industry to produce SiO_2 solid layers [1] and are also relevant to propulsion application. The handling of silane is very hazardous because of its pyrophoric nature [2], i.e., spontaneous ignition at ambient conditions by contact with air. A number of accidental combustion events involving silane-based mixtures are reported in the litterature [3]. Among silane-based mixtures, silane-oxygen and silane-air blends have received the largest attention. A number of shock-tube studies have investigated the high-temperature kinetics of silane-oxygen [4, 5] and silane-fuel-oxygen [6–8] mixtures. Laminar flame speed and flammability limits measurements have been performed by Tokuhashi et al. [9]. The spontaneous ignition of silane-air mixtures has been studied in particular by Hartman et al. [10], Tamanini et al. [2] and Ngai et al. [11]. Concerning silane-nitrous oxide mixtures, most studies have used highly diluted mixtures and have focused on gas phase [12–15] and particule growth [1, 16] kinetics. Although Horiguchi et al. [17] have used non-diluted SiH_4-N_2O mixtures to study the flammability limits, there is, to our knowledge, no data on the burning speed of silane-nitrous oxide based mixtures. The purpose of the present study is to investigate experimentally and numerically the effect of silane addition on the laminar burning speed of hydrogen-nitrous oxide mixtures.

2 Materials and methods

2.1 Experimental procedure

The experimental set-up is shown in Figure 1. The burning speed measurements were made in a spherical stainless steel vessel of 250 mm inner diameter. Two quartz windows, 70 mm in diameter and 40 mm thick, are mounted opposite to each other and allow for the visualisation of the flame. During silane combustion, hot silica particules were formed and melted onto the windows. To protect them, smaller diameter glass windows were added to the inside of the main windows. This however reduced the observation time and lowered the frames quality. Prior to experiment, the vessel was evacuated below 2 Pa. The visualisation was achieved with the schlieren method. The flame propagation was recorded by a Kodak high speed camera with an acquisition frequency up to 13500 frames/s. A pulsed Nd-YAG laser was used to ignite the flammable mixtures. Its ouput energy was controlled by varying the laser pulse length and was maintained as low as possible to minimize the effect of input energy on the flame propagation. The laser beam was directed through a small quartz window perpendicular to the two

optical windows and focused on the tip of a molybdenum electrode. The mixture ignited from the hot spot resulting from the laser-metal interaction and the flame expanded spherically from this point. The evolution of the pressure during the experiments was measured using a Kistler piezo-electric pressure transducer. The uncertainty on the peak pressure is estimated to be 3%.

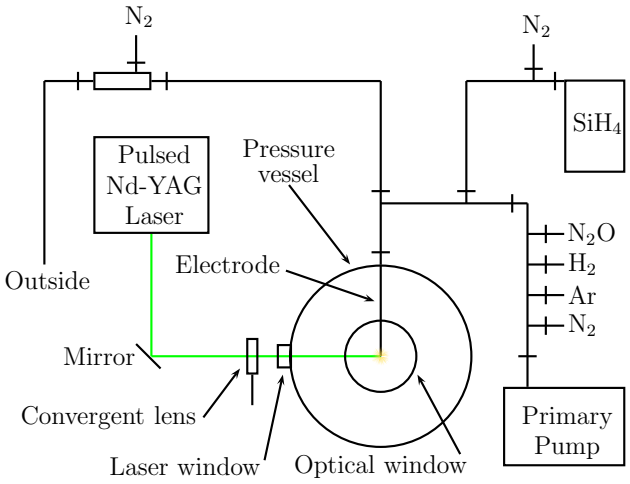

Figure 1: Schematic of the experimental set-up.

Silane-hydrogen-nitrous oxide-argon mixtures were prepared using the partial pressure method from research-grade pure gases. The Ar dilution was held constant at 60% for safety reasons, and the equivalence ratio, Φ, was varied between 0.3 and 2.4. In all experiments, the initial temperature was between 296 and 305 K and the pressure was 51 kPa. In the case of H_2-N_2O mixtures, Φ is simply defined as the ratio of hydrogen molar fraction to nitrous oxide molar fraction. In the case of mixtures containing silane, the two following chemical reactions are considered as defining the stoichiometric combustion:

$$H_2 + N_2O = H_2O + N_2 \tag{1}$$

$$SiH_4 + 4N_2O = SiO_{2(s)} + 2H_2O + 4N_2 \tag{2}$$

The equivalence ratio is defined for a given silane to hydrogen mole fraction ratio, $R_{SiH4/H2}$, and expressed as:

$$\Phi = \frac{X_{H2}}{X_{N2O}} \times \left(1 + 4 \cdot R_{SiH4/H2}\right) \tag{3}$$

Because silane ignites spontaneously when mixed with air, it was not possible to pump down the filling line after silane introduction, so a special system of introduction and evacuation was designed as shown in Figure 1. Silane was introduced within the pressure vessel by successive small amounts (less than 2.5 kPa). When the desired pressure was reached, the remaining silane was pushed with nitrogen into a parallele line until it reached a nitrogen-filled secondary vessel. The mixture was further diluted by a second stream of nitrogen and was evacuated to the atmosphere through a 1 mm diameter hole.

2.2 Flame speed measurement

In the framework of the asymptotic theory [18], the unstretched flame speed can be derived from spherically expanding flame experiments and is given by the following expression:

$$V_S = \frac{dR_f}{dt} = V_S^0 - L \cdot K \tag{4}$$

where: V_S and V_S^0 are the stretched and unstretched laminar flame speed, respectively [m/s]; R_f is flame radius [m]; t is the time [s]; L is the Markstein length [m]; and K is the stretch rate [1/s].
The stretch rate is obtained from the following equation:

$$K = \frac{1}{A}\frac{dA}{dt} = \frac{1}{R_f^2}\cdot\frac{dR_f^2}{dt} = \frac{2}{R_f}\cdot\frac{dR_f}{dt} = 2\cdot\frac{V_S}{R_f} \tag{5}$$

where: A is the flame area [m^2].
Combining Equation 4 and Equation 5 and integrating for $R_f \ll D_{exp}$, where D_{exp} is the characteristic dimension of the experimental set-up, the unstretched flame speed with respect to time and the flame radius is:

$$V_S^0\cdot(t_F - t) = R_{f,F} - R_f + 2\cdot L\cdot ln\left(\frac{R_f}{R_{f,F}}\right) + Cst \tag{6}$$

where: the subscipt F designates the final data point taken into account, and Cst is an integration constant [m].
The unstretched laminar burning speed, S_L^0, is then obtained by dividing the unstretched flame speed by the expansion ratio, σ, which corresponds to the fresh gas density to the burned gas density ratio. A Matlab routine was used to obtain the flame radius as a function of time and a linear least-squares regression was applied to derive V_S^0. Because of the second window added to protect the quartz windows, the accuracy of the flame edge detection is reduced and the uncertainty on S_L^0 is estimated to be 10%.

2.3 Kinetic modeling

The detailed kinetic scheme used in the present study was that of Mével et al. [12]. It is composed of 431 reactions and 92 species. The formation of silicon containing condensed combustion products, SiO(s) and SiO_2(s), is included as described by Suh et al. [19]. The modeling of the laminar burning speed was achieved using the Regath software [20]. Regath is a Fortran 90 package including thermodynamics and chemical routines. It also includes 0-D reactors solvers as well as a 1-D freely-propagating flame solver and a counterflow solver. All the programs of Regath package work for both perfect and real gas conditions. The gases are considered as perfect for all cases studied here.

3 Results and discussion

Figure 2 shows an example of a flame propagation sequence in stoichiometric H_2-N_2O-Ar (a) and SiH_4-H_2-N_2O-Ar (b) mixtures. Figure 3 (a) summarizes the results obtained for the different silane to hydrogen ratios investigated, $R_{SiH4/H2}$=0, 1/3, 1 and 3. The addition of silane in hydrogen-nitrous oxide mixtures induces a significant increase of the burning speed. For example, at Φ=1, replacing 25% of hydrogen by silane, $R_{SiH4/H2}$=1/3, results in an increase of 31% in the burning speed. Above $R_{SiH4/H2}$= 1, the burning speed remains essentially independant of the silane content, within the uncertainty of the measurements. The increased burning speed might be explained by the flame temperature increase with silane addition and possibly by faster chemical pathways. Both effects lead to higher energy release rates which overcome the decrease of the thermal diffusivity induced by silane addition. The predictions of the detailed reaction model are shown as solid lines in Figure 3 (a). Good agreement is found for all silane content for lean, stoichiometric and rich mixtures up to Φ= 1.2. For the richer mixtures, the model predicts accurate burning speed only at low silane content. Above $R_{SiH4/H2}$= 1, the overprediction of experimental data by the model increases with silane content.
Figure 3 (b) shows the measured peak pressures along with constant volume explosion calculations obtained both with and without including the thermodynamic properties of condensed combustion products. Increasing the amount of silane results in an increase of the peak pressure as well as a shift of the maximum value toward higher equivalence ratios. Whereas for H_2-N_2O-Ar mixtures, the measured peak pressure is within 5% of the theoretical values, much larger differences are observed for mixtures containing silane. For SiH_4-H_2-N_2O-Ar mixtures, the difference between experimental and ideal values

increases with increasing silane content, from 11% at $R_{SiH4/H2}$= 1/3 up to 17% at $R_{SiH4/H2}$= 3, and with equivalence ratio, from about 1% at Φ=0.3 up to 30% at Φ=2.6 for $R_{SiH4/H2}$= 3. If the condensed combustion products are not included to calculate the constant volume peak pressure, the difference between the measurements and the ideal values is very low, 3% in average. The simplified CV calculation does not account for the change in the mass of gas due to the condensation of the SiO_2 products, which may partly explain the large differences between observed and computed peak pressures.

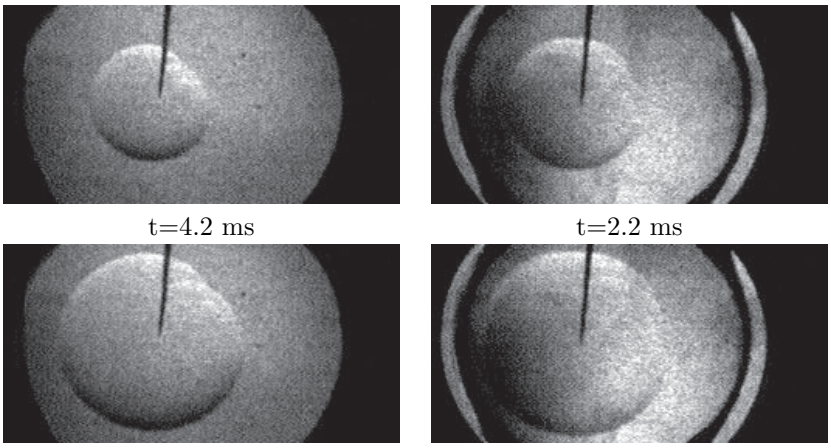

(a): H_2-N_2O-Ar (b): SiH_4-H_2-N_2O-Ar

Figure 2: Example of schlieren images obtained with stoichiometric H_2-N_2O-Ar (a) and SiH_4-H_2-N_2O-Ar (b) mixtures. Initial conditions: (a): X_{Ar}=0.6; T_1=302 K; P_1=51 kPa. (b): $R_{SiH4/H2}$= 1/3; X_{Ar}=0.6; T_1=305 K; P_1=51 kPa.

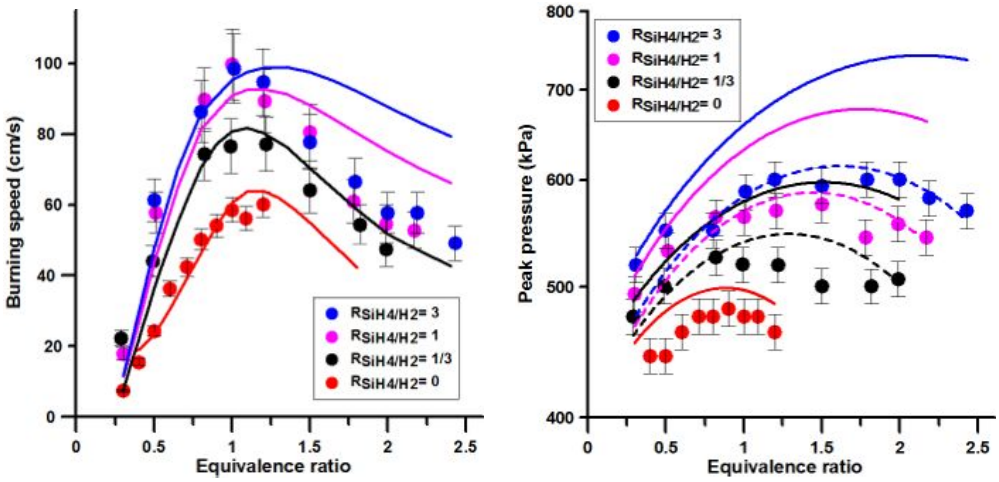

(a) Burning speed (b) Peak pressure

Figure 3: Experimental and numerical (a) burning speed and (b) peak pressure for H_2-N_2O-Ar mixtures with and without SiH_4. Initial conditions: X_{Ar}=0.6; T_1=300 K; P_1=51 kPa. In (b), the solid and dashed lines correspond respectively to the calculated peak pressure obtained with and without condensed combustion products.

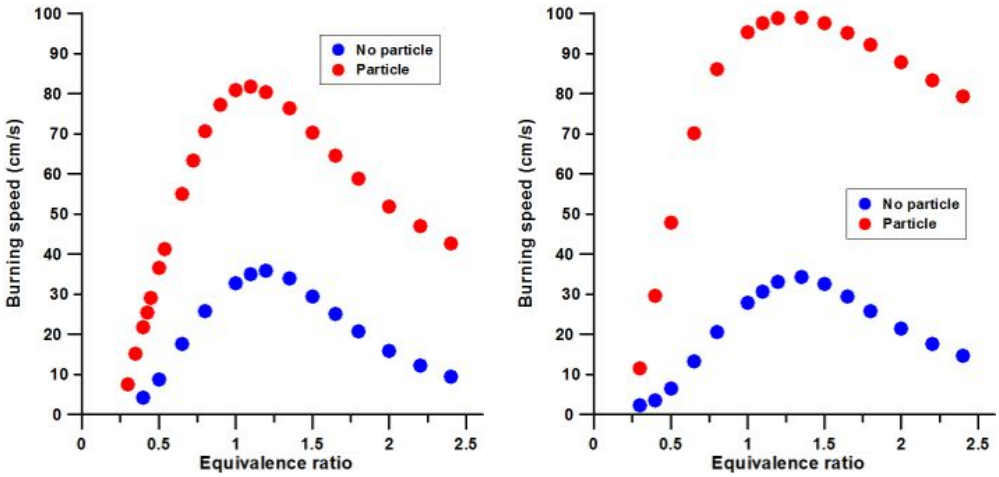

(a) $R_{SiH4/H2}$=1/3 (b) $R_{SiH4/H2}$=3

Figure 4: Numerical burning speed for SiH_4-H_2-N_2O-Ar mixtures with and without particle formation. Initial conditions: X_{Ar}=0.6; T_1=300 K; P_1=51 kPa.

In order to investigate the influence of silica particle formation on the flame propagation, two series of calculations have been performed. In the first one, the reaction pathways leading to the formation of condensed particules have been included whereas in the second series, these pathways have been omitted. Figure 4 shows the results of these calculations for $R_{SiH4/H2}$= 1/3 and 3. For all SiH_4 to H_2 ratios, the calculated burning speed is much higher when the formation of condensed silica particles is included. This result emphasizes the important role of condensed particle formation in the energy release rate during silane-based mixtures combustion and is consistent with the observation of Babushok et al [21] who studied the burning speed of silane-oxygen-nitrogen mixtures. However, as the pressure measurements show, a significant amount of the energy released by the particle formation is lost. We believe this is due to heat losses associated with thermal radiation from the growing silicon oxide particles. In addition, the simplified nature of the model used to describe the formation of condensed combustion products, including inacurracy in the thermodynamic data, could contribute to the differences observed.

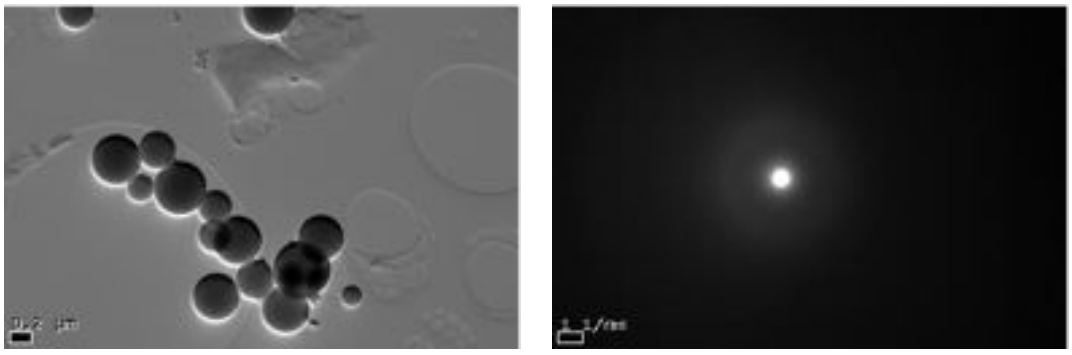

(a) TEM image (b) Diffraction pattern

Figure 5: Transmission electron microscopy image (a) and electronic diffraction pattern (b) obtained for solid particles formed during a SiH_4-N_2O-Ar mixture combustion. Initial conditions: Φ=1.79; X_{Ar}=0.6; T_1=300 K; P_1=101 kPa.

Figure 5 presents transmission electron microscopy image and electronic diffraction pattern obtained for these particles. The particles appear as nano-spheres with an average diameter of 350±142 nm. The

diffraction pattern demonstrates that these particles are amorphous. Energy dispersive X-ray spectroscopic analysis shows that the particles are mainly composed of Si and O atoms and further work is in progress to better characterize the particles composition.

4 Conclusion

The burning speed of hydrogen-silane-nitrous oxide has been experimentally and numerically investigated. It was shown that the addition of silane results in a significant increase of the burning speed up to $R_{SiH4/H2}$=1. The detailed kinetic model demonstrated overall agreement with the experimental results. The simulations also showed that the formation of condensed particules appears to play a significant role in the propagation of flames in silane-based mixtures. Future work will focus on estimating radiative processes and the effects of heat losses on the flame propagation.

References

[1] Giunta C., Chapple-Sokol J. and Gordon R. (1990). Journal of the Electrochemical Society 137: 3237.

[2] Tamanini F., Chaffe J. and Jambar R. (1998). Process Safety Progress 17: 243.

[3] Hirano T. (2004). Journal of Loss Prevention in the Process Industries 17: 29.

[4] Petersen E. et al. (2004). Proceedings of the International Symposium on Shock Waves 24: 585.

[5] Mick H.-J. (1995). PhD thesis: University of Duisburg.

[6] Petersen E., Kalitan D. and Rickard M. (2004). Journal of Propulsion and Power 20: 665.

[7] Rickard M., Hall J. and Petersen E. (2005). Proceedings of the Combustion Institute 30: 1915.

[8] McLain A., Jachimowski C. and Rogers R. (1983). NASA report.

[9] Tokuhashi K. et al. (1990). Combustion and Flame 82: 40.

[10] Hartman J. et al. (1987). Combustion and Flame 68: 43.

[11] Ngai E. et al. (2007). Process Safety Progress 26: 265.

[12] Mével R., Javoy S. and Dupré G. (2011) Proceedings of The Combustion Institute 33: 485.

[13] Javoy S., Mével R. and Dupré G. (2010). Chemical Physics Letters 500: 223.

[14] Becerra R. et al. (1991). Chemical Physics Letters 185: 415.

[15] Mick H. and Roth P. (1994). Journal of Physical Chemistry 98: 5310.

[16] Chapple-Sokol J., Giunta C. and Gordon R. (1988). Proceedings of the Materials Research Society Symposium 105: 127.

[17] Horiguchi S. et al. (1989). Koatsu Gasu 26: 840.

[18] Clavin P. (1985). Progress in Energy and Combustion Science 11: 1.

[19] Suh S.M., Zachariah M. and Girshick S. (2001). Journal of Vacuum Science and Technology A 19: 940.

[20] Candel S., Schmitt T. and Darabiha, N. (2011). Proceedings of the 23^{rd} ICDERS.

[21] Babushok V. et al. (1998). Proceedings of The Combustion Institute 27: 2431.